LARGE EDDY SIMULATION OF FLAMEHOLDER-STABILIZED WITH TURBULENT PREMIXED FLAME

Nicolas Moises Cruz Salvador nicase03@yahoo.es
Wladimyr Mattos da Costa Dourado.wladimyr@iae.cta.br
Combustion and propulsion Laboratory (LCP)/INPE Rod. Presidente Dutra Km. 40 Cachoeira Paulista – SP – CEP 12630-000
Institute of Aeronautics and Space(IAE) Space Propulsion Division (APE). Praça Mal. Eduardo Gomes 50 Vila das Acácias São José dos Campos – SP – CEP 3941-2333 +55 (12) 3947-4717
Marcio Texeira MendonçaThird Author's Name, e-mail
Instituto Tecnico Aeronautico (ITA) Praça Mal. Eduardo Gomes 50 Vila das Acácias São José dos Campos – SP – CEP 3941-2333 +55 (12) 3947-5169

Abstract. *The simulation of a turbulent reacting flow in a channel with obstacle carried out experimentally, was reproduced using a numerical model with large eddy simulation, with turbulent and combustion model for premixed flame Xi, present in OpenFOAM. Both inert flows and reactive flows simulations were performed. In the inert flow, comparison with velocity profile and recirculation vortex zone in unsteady flow was performed, as well as an analysis of the energy spectrum obtained numerically. The spectrum was obtained in order to confirm if the mesh is adequate for the turbulence models adopted. The simulation with reacting flow considered a pre-mixture of propane (C3H8) with air such that the equivalence ratio was equal to 0.65, with a theoretical adiabatic flame temperature of 1800 K. The results show good agreement with the experimental data.*

Keywords: *LES, Turbulent combustion, finite volume, reactive flow.*

1. INTRODUCTION

In the context of turbulent reactive flow simulation, models have achieved a great development in recent years with the improvement of computer power. This development allowed more accurate solutions of problems such as instability caused by thermoacoustic coupling in combustion chambers of rocket engines and gas turbines. On the other hand, in analysis of turbulent combustion and models for such phenomena is observed that the behavior of the turbulent flame front is predominantly dictated by the turbulence (Peters, 2000).

Added to this the fact that the phenomena of combustion instability are directly related to interaction with turbulence combustion, and these to acoustics (Wolf *et al.*, 2009). Therefore it becomes mandatory that the turbulence model be able to reproduce these dynamic processes, which are mainly produced by large scale turbulene. In this sense the purpose of this study is to evaluate the OpenFOAM open source software, which contains turbulence models for large eddy simulation (LES) and premixed turbulent flames, to simulate a turbulent flow, inert and reactive. It is proposed to compare the numerical results of the present work with experimental results obtained by Sanquer (1998).

In this paper we present results of numerical simulations with LES in two and three dimensions in order to simulate inert and reactive flows an compare with experimental results obtained by Sanquer (1998). The two cases consist of a flow channel of rectangular cross section with triangular section obstacle and the Reynolds number, based on the side of the triangle equal to 6690. We tested several types of meshes and various types of turbulence models to see which performs better in the simulation compared with experimental values.

Many researchers have been conducted Reynolds Averaged Navier Stokes (RANS) methods for reactive flows behind bluff bodies, but important discrepancies were observed due to shortcomings inherent in the RANS methodology, especially in complex flows (Bai and Fuchs, 1994; Dourado, 2003). In LES, the three dimensional large scale motion is resolved, hence the non-universal, geometry dependent flow features are captured accurately, and only the small scales that exhibit local isotropy are modelled, Porumbel (2006) who development the bluff body with the Linear Eddy Mixed (LEM) model in premixed Flame, founded good agreement with the experimental.

2. Problem Formulation

The Favre filtered LES equations are Fureby (2009):

$$\begin{cases} \partial_{\mathbf{t}}(\overline{\rho}) + \nabla \cdot (\overline{\rho}\tilde{\mathbf{v}}) = \mathbf{0}, \\ \partial_{\mathbf{t}}(\overline{\rho}\tilde{\mathbf{Y}}_{\mathbf{i}}) + \nabla \cdot (\overline{\rho}\tilde{\mathbf{v}}\tilde{\mathbf{Y}}_{\mathbf{i}}) = \nabla \cdot (\bar{\mathbf{j}}_{\mathbf{i}} - \mathbf{b}_{\mathbf{i}}) + \overline{\dot{\omega}_{\mathbf{i}}}, \\ \partial_{\mathbf{t}}(\overline{\rho}\tilde{\mathbf{v}}) + \nabla \cdot (\overline{\rho}\tilde{\mathbf{v}} \otimes \tilde{\mathbf{v}}) = -\nabla\overline{\mathbf{p}} + \nabla \cdot (\overline{\mathbf{S}} - \mathbf{B}), \\ \partial_{\mathbf{t}}(\overline{\rho}\tilde{\mathbf{E}}) + \nabla \cdot (\overline{\rho}\tilde{\mathbf{v}}\tilde{\mathbf{E}}) = \nabla \cdot (-\overline{\mathbf{p}}\tilde{\mathbf{v}} + \tilde{\mathbf{S}}\tilde{\mathbf{v}} + \overline{\mathbf{h}} - \mathbf{b}_{\mathbf{E}}), \end{cases} \tag{1}$$

The filtered LES equations have terms that reflect the effects of unresolved scales on resolved scales of motion, and the result of the filtering processes are here denoted by the terms $\mathbf{B}$, $\mathbf{b_i}$ and $\mathbf{b_E}$. Also $-$ and $\sim$ represent the spatially filtered

quantities and Favre averages respectively, ρ is the density, $\mathbf{v}$ the velocity p thconcordane pressure, $\mathbf{S}$ are the stress viscous tensor, $\mathbf{E} = h - p/\rho + \frac{1}{2}\mathbf{v^2}$ represent the energy, h entalphy $\mathbf{h}$ is the heat flux vector and $\mathbf{Y_i}$, $\mathbf{j_i}$ and $\dot{\omega}_i$ the weigth fraction, difussion weigth and the reaction rate of ith species. In sum, the equations of filtered Navier-Stokes contains several terms without closing that must be modeled:

$$\begin{cases} \mathbf{B} = \overline{\rho}(\widetilde{\mathbf{v} \otimes \mathbf{v}} - \tilde{\mathbf{v}} \otimes \tilde{\mathbf{v}}) \\ \mathbf{b_i} = \overline{\rho}(\widetilde{\mathbf{v}\mathbf{Y_i}} - \tilde{\mathbf{v}}\tilde{\mathbf{Y}}_\mathbf{i}) \\ \mathbf{b_E} = \overline{\rho}(\widetilde{\mathbf{v}\mathbf{E}} - \tilde{\mathbf{v}}\tilde{\mathbf{E}}) \end{cases} \tag{2}$$

On the basis Grinstein and Kailasanatha Grinstein and Kailasanath (1994) assumed that the gas mixture viscosity is linear, with heat conduction according to Fourier law and diffusion by Ficks law, the constitutive equations and the level of sub-grid:

$$\overline{\mathbf{S}} \approx \mathbf{2}\mu\tilde{\mathbf{D}}_\mathbf{D} \tag{3}$$

where $\mathbf{D_D}$ is the deviatoric part of $\tilde{\mathbf{D}} = \frac{\mathbf{1}}{\mathbf{2}}(\nabla\tilde{\mathbf{v}} + \nabla\tilde{\mathbf{v}}^\mathbf{T})$

$$\overline{\mathbf{h}} \approx \mathbf{k}\nabla\tilde{\mathbf{T}} \tag{4}$$

$$\bar{\mathbf{j}}_\mathbf{i} \approx \mathbf{D_i}\nabla\tilde{\mathbf{Y}}_\mathbf{i} \tag{5}$$

The state equation are:

$$\overline{\mathbf{p}} \approx \overline{\rho}R\tilde{T}\sum_i(\tilde{Y}_i/M_i) \tag{6}$$

Where $\tilde{T}$ is the temperature and R is the gas constant. The viscosity, μ is modeled by Suterland's law and species and thermal diffusivities are $D_i = \mu/Sc_i$ and $k = \mu/Pr$, respectively, where Sc and Pr are the Schmidt numbers and Prandtl numbers respectively. The total energy filtered result in:

$$\tilde{E} = \overline{h} - \overline{p}/\overline{\rho} + \frac{1}{2}\tilde{\mathbf{v^2}} + k \tag{7}$$

Also $k = 1/2(\widetilde{\mathbf{v^2}} - \tilde{\mathbf{v^2}})$ that is the cinetic energy of sub-grid and the filtred:

$$\tilde{h} = \sum_i(\tilde{Y}_i h^\theta_{i,f}) + \sum_i(\tilde{Y}_i \int_{T0}^{\tilde{T}} C_{p,i}(T)dT) \tag{8}$$

from which $\tilde{T}$ results.

2.1 Combustion model

To close these equations we need models for the sub-grid scale (SGS) stress tensor, flux vectors, dissipation and reactions rates. A one-equations eddy-viscocity model is used in this study (Fureby *et al.*, 1997). This model based in flamelets, in wich the flame is considered thin compared to the length scales of the flow, and is hence an interface between reactants and products. Using a conditional filtering to generate transport equations that differs from conventional models that use the flame surface density, generate a surface function Ξ called wrinkling surface, which is the flame surface area per unit area resolved in the mean direction of propagation. The principle difficulty in reacting LES is the proper treatmen of the reaction zone; since the characteristic scales for the reactions processes are below the filter width, them, mean reaction rate models are required. By conditioning the continuity equation, treating only unburned gases state before filtering, we obtain a transport equation for the resolved part of the unburned gas mass fraction, or regress variable $\tilde{b}$ (Weller *et al.*, 1998). Also the velocity $\mathbf{v}$ been changed to U and for this model becomes, $U_I = U + v_a n_\perp$ where U_I is the full velocity on an interface consisting of the movement due to advection term and the advance of the interface relative to the flow.

$$\frac{\partial\overline{\rho}\tilde{b}}{\partial t} + \nabla.(\overline{\rho}\tilde{U_u}\tilde{b}) = -\overline{\rho}_u S_u \Xi|\nabla\overline{b}| \tag{9}$$

Where $-$ and $\sim$ represent variables filtered and weighted by the density respectively. The volumetric fraction of unburnt gas $\overline{b}$ is related to $\tilde{b}$ by $\overline{\rho_u}\overline{b} = \overline{\rho}\tilde{b}$ and Ξ is a sub-grid flame wrinkled, and has also modeled the forward term of the interface on the flow $\widetilde{\rho v_a}$ resulting in the filtering process in terms of laminar flame speed S_u and unburned gas density ρ_u. The conditional filter of unburned gas velocity $\tilde{u_u}$is modeled using $\tilde{U_U} = \tilde{U} + (1 - \tilde{b})\overline{U}_{ub}$ where $\overline{U}_{ub}$ is the

slip velocity of the unburned less burned gas $\overline{U}_{ub} = \overline{U}_u - \overline{U}_b$ by analogy with the properties of laminar flame can get a connection for use with LES:

$$\overline{U}_{ub} = (\frac{\overline{\rho}_u}{\overline{\rho}_b} - 1)S_u \Xi \hat{n} - D\frac{\nabla\tilde{b}}{\tilde{b}(1-\tilde{b})} \tag{10}$$

Being D the diffusion coefficient of the sub-grid, and the flame normal $\hat{n} = \nabla\tilde{b}/|\nabla b|$, combining Eq. (9) and (10) we arrive at equation modeled to $\tilde{b}$, (Weller and Tabor, 2004):

$$\frac{\partial\overline{\rho}\tilde{b}}{\partial t} + \nabla.(\overline{\rho}\tilde{U}\tilde{b}) - \nabla.(\overline{\rho}D\nabla\tilde{b}) = -\overline{\rho}_u S_u \Xi|\nabla\tilde{b}| \tag{11}$$

The transport equation for the sub-grid flame area density Σ proposed by Weller (1993) is obtained from the relation $\Xi = \Sigma/|\nabla\bar{b}|$ and the resolved unburned gas volume fraction b. The transport equation for the flame wrinkled is:

$$\frac{\partial\Xi}{\partial t} + \widetilde{U_s}.\nabla\Xi = -\overbrace{n.(\nabla U_s).n}\,\Xi + \hat{n}(\nabla\widetilde{U_t})\hat{n}\Xi + (\widetilde{U_t} - \widetilde{U_s}).\frac{\nabla|\nabla b|}{|\nabla b|}\Xi \tag{12}$$

Where $\widetilde{U_t}$ is the surface-filtered effective velocity of the flame defined by $\partial\bar{b}/\partial t + \widetilde{U_t}\,\nabla\bar{b} = 0$ and U_s is the local instantaneous velocity of the surface flame. The first and second term on the right side of Eq. (12) represent the effects of stress and propagation on the SGS of wrinkled Ξ. The third term on the right side of Eq. (12) represent the effects of strain and propagation differential on Ξ through the flame, reducing the generation at the front of the flame and increasing the generation at the back. These terms involve higher order derivatives and create numerical difficult for LES and are avoided. Rather than attempting to model for each term in detail models representing the generation and removal of wrinkled, are modeled respectively by $G\Xi$ and $R(\Xi - 1)$. The problem associated with these derivatives is thus avoided by including the effect directly into the model for a given value of G, resulting in the following simplified equation for Ξ:

$$\frac{\partial\Xi}{\partial t} + \widetilde{U_s}.\nabla\Xi = G\Xi - R(\Xi - 1) + (\sigma_s - \sigma_t)\Xi \tag{13}$$

Here the final term may be correlated with the strain rates resolved
$\sigma_t = \frac{1}{2} \parallel \nabla\widetilde{U_t} + \nabla\widetilde{U_t}^T \parallel$ and $\sigma_t = \frac{1}{2} \parallel \nabla\widetilde{U_I} + \nabla\widetilde{U_I}^T \parallel$.

The values for the parameters G and R should be modeled. A spectral approach is applied to the modeling of turbulent flame interaction in which the wrinkled flame front is represented by a distribution of length-scale distortions of the surface, limited by the size of the flame kernel and laminar flame thickness (Weller *et al.*, 1990). However, the solution of the equations of spectral evolution coupled with the transport equations for Ξ is expensive and algebraic models are considered more appropriate. The approach is based on the correlation of Gülder for flame speed (Gulder, 1990):

$$G = R\frac{\Xi_{eq} - 1}{\Xi_{eq}},\ R = \frac{0.28}{\tau_\eta}\frac{\Xi^*_{eq} - 1}{\Xi^*_{eq}} \tag{14}$$

Where the results are in agreement with the experiments.

$$\Xi^*_{eq} = 1 + 0.62\sqrt{\frac{u'}{S_u}}Re_\eta, \tag{15}$$

$$\Xi_{eq} = 1 + 2(1-b)(\Xi^*_{eq} - 1) \tag{16}$$

τ_η is the Kolmogorov time, u' is the intensity of turbulence in the sub-grid and Re_η is the Reynolds number of Kolmogorov. It is assumed that the laminar flame speed is in balance with the rate of local deformation and in linear response, resulting:

$$S^\infty_u = S^0_u max(1 - \sigma_s/\sigma_{ext}, 0) \tag{17}$$

where σ_{ext} is the strain rate at extinction. Unfortunately, the scales of chemical time of poor flame, can be comparable to the time scales of deformation and transportation, making this case that the local equilibrium assumption is wrong, and then requested a full transport equation. By analogy with the transport of a wrinkled flame, it is expected that the filtered laminar flame speed, is carried by the surface speed of flame filtered $\widetilde{U_s}$. Assuming that the timescale of strain rate is $1/\tau_s$ and chemical time scale is such that, when $t \to \infty, Su \to S^\infty_u$ then:

$$\frac{\partial S_u}{\partial t} + \widetilde{U_s}.\nabla S_u = -\sigma_s S_u + \sigma_s S^\infty_u \frac{(S^0_u - S_u)}{(S^0_u - S^\infty_u)} \tag{18}$$

Thus, the wrinkled flame model can be simplified by replacing Ξ in Eq. (13) by the equilibrium Eq. (16) and also by substitution in Eq. (18), by Su equilibrium Eq. (17).

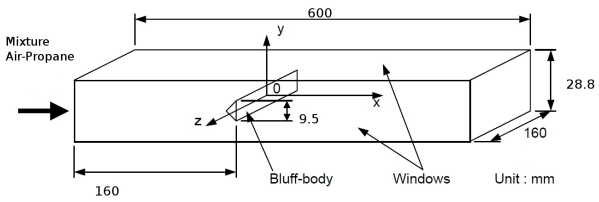

Figure 1. Scheme of the experimental channel with obstacle of Sanquer (1998).

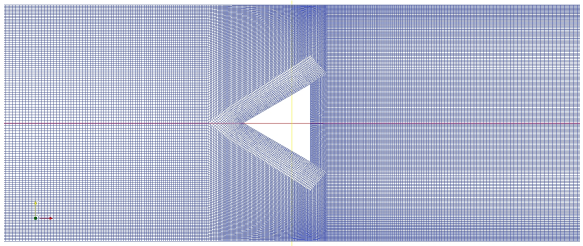

Figure 2. Grid structure with better performance computing around of the obstacle.

3. NUMERICAL MODEL

The LES filtered Navier-Stokes Eq. (1), together with the sub-grid kinetic energy transport Eq. 18) are solved using a finite volume. The model using explicit time discretization. The turbulence models used in the present work was Smagorinsky model originally available in the code. The solver considers the Navier-Stokes equations how compressible flow, which is the appropriate approach to flow with combustion. For spatial discretization schemes used are second and third order TVD (Total Variation Diminishing) and Euler's method for time discretization. All implemented in the algorithm PISO (pressure-implicit split-operator) to solve the pressure-velocity coupling. The discretization method code is the standard adopted by the Gauss integration for finite volume. This report was developed as a specific combustion solver called Xifoam. This premixed combustion models or partially premixed turbulent combustion were described before (Weller *et al.*, 1998; Weller and Tabor, 2004).

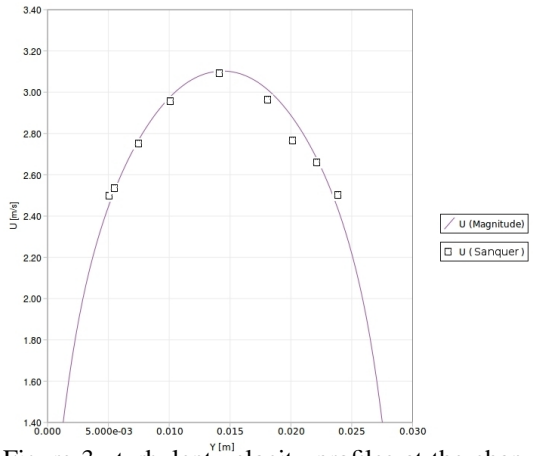

Figure 3. turbulent velocity profiles at the channel entrance, experimental and imposed as initial condition.

3.1 Initials and boundary conditions

The model studied, consists of a channel of 600 cm, long, 160 cm, wide and 28.8 cm in height, where the flow turbulent has a Reynolds of 6600 in entrance section of the channel. The obstacle used as flame holder his equilateral triangular cross section whose back side is located 160 cm from the entrance, the transverse dimension is such that the obstacle blocking the flow in 33% of the total area and corresponding to r-65 in the Sanquer Thesis. Figure 1 shows the topology of the channel. In the first part of the simulation flow is only inert and initial temperature is 300 K, it is considered that the outlet of the channel is open but adds a wave of "transmissivity" for pressure control (Candel, 1992), a turbulent velocity profile is imposed at the entrance with a speed of 3.1 m / s as shown in Fig. 2. A wall function in the chanel walls and the obstacle is used Jayatilleke (1969). The second part of the simulation corresponds to the reacting flow. Propane (C3H8) is added premixed with air and it is ignited is behind the obstacle in the recirculation zone to achieve a proper performance and avoid extinction. The initial flame speed is 0.256 m/s. regress variable b is equal to (c-1) with given value for gases not burned, so early in the whole field is considered 1.

Several types of mesh were built and tested to evaluate the computational performance, and the mesh presented in this paper achieved the better results. It is composed of 388,355 volumes in the mesh in two-dimensional field and 2300,000 volumes in 3D discretization. Figure 2 shows mesh details around the obstacle. The instantaneous velocity of flow was taken to determine where him can be taken as periodic stationary. Figure. 4 shows the history of longitudinal velocity and axial flow and Fig. 5 the transversal component. As we can see the transition lasts until 18 milliseconds, so the flow can

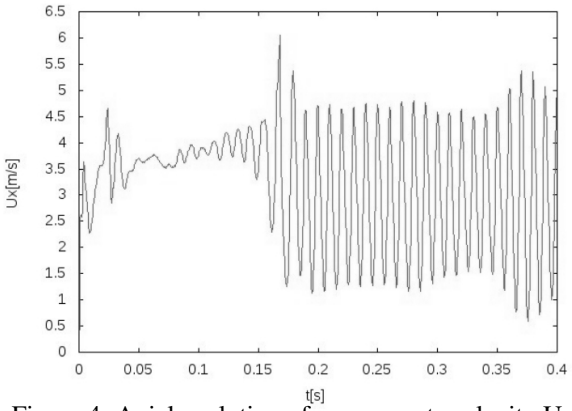

Figure 4. Axial evolution of components velocity Ux

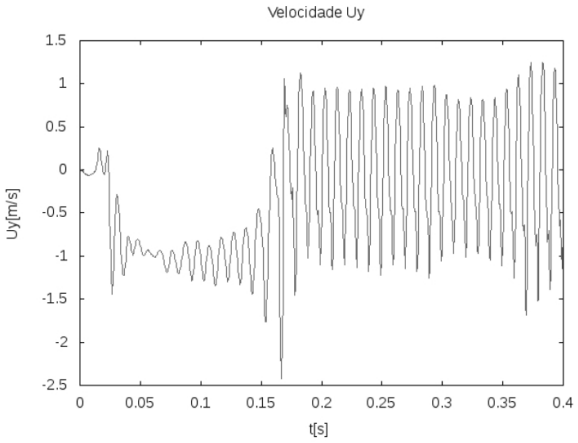

Figure 5. Transversal evolution of component velocity Uy

be considered stationary periodical.

4. RESULTS

To determine the recirculation zone becomes the measures of velocity components from the time that experiment reaches the stationary regime periodico, as well as to obtain the energy spectra. Once we determine the length of the the recirculation zone, we can determine by calculating the Strouhal number to compare with experimental results. To determine the values of the energy spectrum we take the Fast Fourier transform FFT of oscilatory velocity mean with the power to determine if we are able to simulate the large scales and the scales of sub-grid. In the reactive case is implemented an ignition point at 0.05 m behind the obstacle in the center of the recirculation zone that ensures no flame extinction, the combustion time was 0.3 sec.

Table 1. Comparison of results LES and RANS simulation vs experimental.

Case	$f_q[Hz]$	$f_q d/U_{axe}$	$\triangle x_L[m]$	x_L/d
Experiments Sanquer	89	0.276	0.0204	2.12
LES current work	93.5	0.284	0.023	2.42
RANS (Dourado, 2003)	87	0.2694	0.0222	2.31

4.1 Inert flow case

The Strouhal number, defined as $St = f_q d/U_a xe$ is found to be equal to 0.294, in good agreement with earlier numerical and experimental studies. In the above, $f_q d$ is the shedding frequency, d is size of the bluff body, and U_{axe}

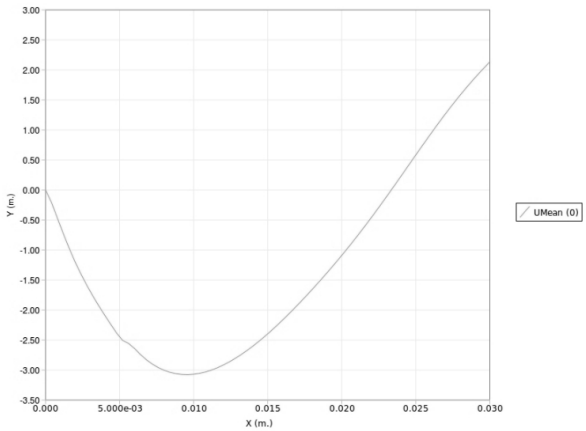

Figure 6. Axial evolution of the average longitudinal component velocity $\tilde{u}$ in present work.

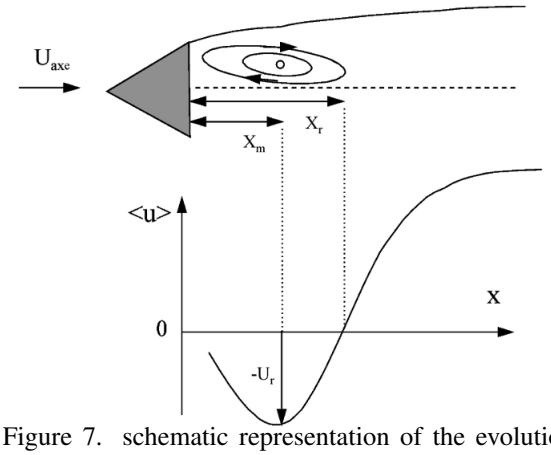

Figure 7. schematic representation of the evolution of velocity Sanquer Sanquer (1998)

is the inflow velocity, 3.1 m/s. The analysis show good agreement with those obtained experimentally as show Tab. 1.

The Strouhal number of emission of vortices is 96% of that obtained experimentally. Also, the recirculation length differs approximately 11.5% from the experimental value. There exist a strong dependence of these parameters on the turbulence model and boundary conditions Veynante (2006). The figure 6 presents the normalized time-averaged axial velocity profile along the combustor centerline, behind the bluff body. The numerical result matches closely the experimental data. Immediately downstream of the bluff body, the velocity is negative and reaches a negative maximum of about 64% of the inflow velocity at Xm. The length of the recirculation region is in Xr Sullerey *et al.* (1975). After the end of the reverse flow area, the mean axial velocity increases upstream to gradually approach the free stream value, as the velocity deficit induced by the bluff body disappears. The length of recirculation zone based on the evolution of the average velocity Ux in a unsteady periodic regime, were determined. This process consists in taking the average values along the X axis of the channel immediately after leaving the back of the obstacle. The fig. 6 shows the profile of the average velocity that is known as recirculation zone, the value found is 0.023 m. However the one found by Sanquer (1998) is 0.0204. To determine the emission frequency of the vortices we use a Fourier temporal analysis Dourado (2003), the value 93.5 Hz is captured for a Strouhal number St = 0.284, which compared with the experimental St = 0.276 differs only 3%. It indicated that numerical values are close to the experimental. The Table 1 resume numerical and experimental global parameters. Here is possible see that the results obtained in LES simulation are in corcondance with those obtained with RANS simulation and also in relation to the experimental.

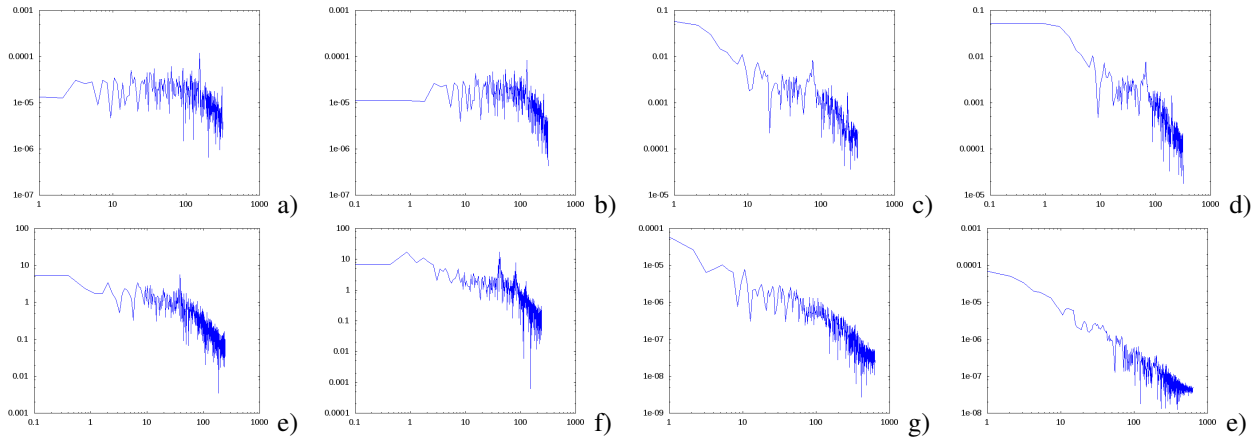

Figure 8. Energy spectrum of longitudinal and transversal velocity components in a)Ux $x/Xr = 1.4$; $y/h = 0$. b) Ux in x/Xr; $y/h = 0.41$ c) Uy in x/Xr ;$y/h = 0$ d) Uy in x/Xr ;$y/h = 0.41$.e)3-D Ux in $x/Xr = 1.4$; $y/h = 0$. f)3-D Uy in $x/Xr = 1.4$; $y/h = 0.41$. g)Energy spectrum of cross component of velocity 3-D Uxy in $x/Xr = 1.4$; $y/h = 0$. e)Energy spectrum of transverse component of velocity 3-D Uz in $x/Xr = 1.4$; $y/h = 0.41$.

The values for the energy spectrum are shown in fig. 8 at two points for the longitudinal and transverse components of velocity in concordance with fig. 7 scheme. As in the work of Sanquer (1998), these points are in $X/Xr = 1.4$; $Y/h = 0$ and $X/Xr = 1.4$ and $Y/h = 0.41$ and as can be seen in all figures, exist a tendency to slope -5/3 and a peak immediately after the 100 Hz, which represents the alternate vortex shedding frequency and compares well with the experimental, this indicate also that size grid is coherent, because the filtered scales is corrected. The model captured this signal and differs from the Experimental for the longitudinal component at$x/Xr = 0$. In the reactive case 3D, In graph (b) away from the

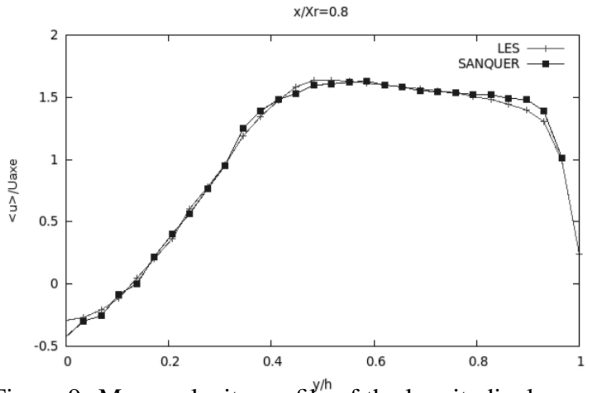

Figure 9. Mean velocity profile of the longitudinal component of velocity Ux in $x/Xr = 0.8$

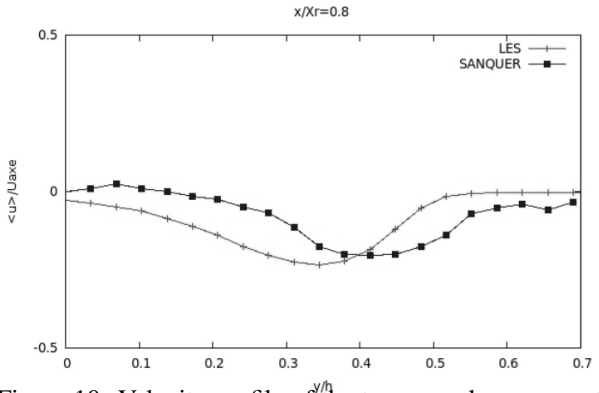

Figure 10. Velocity profile of the transversal component of velocity Uy in $x/Xr = 0.8$

axis the behavior is more consistent, in cases (c) and (d) the behavior is similar. In case 3-D the behavior is more defined as show fig. 8 (e, f g and h) where that besides of the components transverse and longitudinal cross components XY and

Z in the section X / Xr = 1.4 and Y / h = 0. This can be explained because the tensors crossed SGS only be simulated correctly in 3-D.

4.2 Reactive case

In the reactive case 3D, from the results we can see that the model leads to good results and show that the large scales are better represented in the simulation. For the present study on the reactive flow, we compare the values obtained experimentally by Sanquer for case with a triangular dihedral with 33% of the channel blockage and with a equivalence ratio equal 0.65 referred as r1-65. Here we have good agreement between experimental and numerics results, for example the axial velocity at the entrance, with 3.1 m/s development in agreement with the expected if we take into account the margin of error in the experimental is 7% for the velocity profiles. How in inert flow case shows also, transverse profiles of the normalized time-averaged axial and transverse velocities at two locations downstream of the bluff body. As can be seen in Fig. 9 and 11, the profile obtained in the simulation is very close to the experimental longitudinal velocity. For the fig. 10 and 12 the values of transverse velocity component is slightly underestimate in the simulated to the left. However the highest and lowest $Ux/Uaxe$ (0 and -0.2) are within the limits of the experimental. Another results show

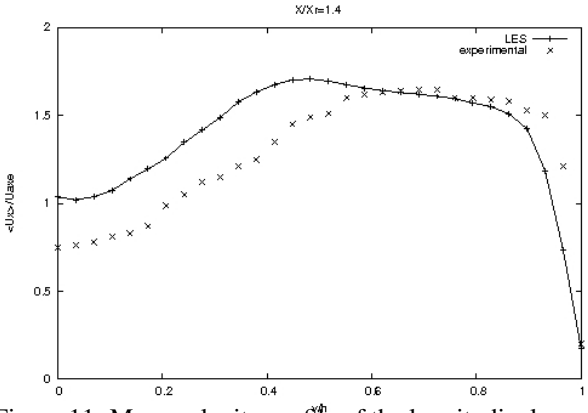

Figure 11. Mean velocity profile of the longitudinal component of velocity Ux in $x/Xr = 1.4$

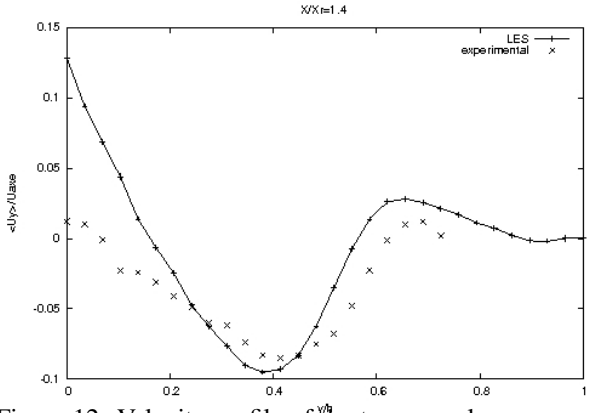

Figure 12. Velocity profile of the transversal component of velocity Uy in $x/Xr = 1.4$

the Fig. 13 where the regress variable is showed, the numeric with the experimental differ overstimated also with a little displacement to the right in the simulation, but the value of 0.4 for $h/y > 0.5$ coincides with the observations made by Sanquer (1998) in the experimental case. In the temperature variable, we obtained a value 1750 K in the average temperature for the configuration of the flame, the value at the Experimental for a reaction rate of 0.65 was 1750 K with flame speed equal to 0.256 m/sg. The results are shows in Fig. 15 where presents the instantaneous temperature.

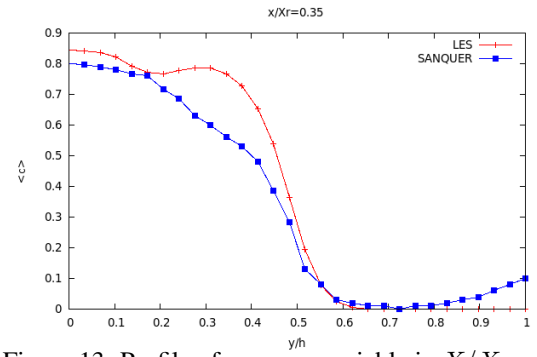

Figure 13. Profile of progress variable in $X/Xr = 0.35$

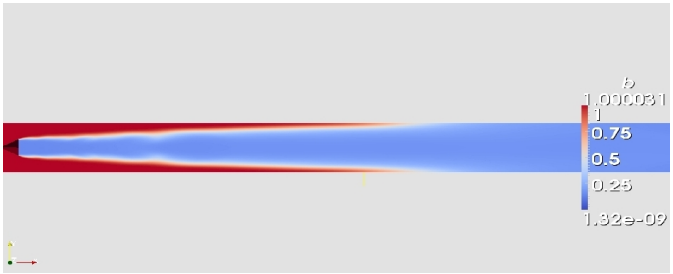

Figure 14. Profile of progress variable in $X/Xr = 0.35$

5. CONCLUSIONS

It was found that OpenFoam can reproduce the experimental data obtained by S. Sanquer and numerical solutions were obtained for 2 and 3 dimensions models. However the values of the energy spectra for 3-D best represented the values -5/3 cascade. This is in agreement with the fact that the LES model is threedimensional, and two dimensional results are actually not allowed. The values for the recirculation zone were reached in the expected range and the Strouhal number is very close to that found in the experiment, as can be seen in Tab. 1. These results are in agreement with the values obtained with a RANS models. The results for the 3-D simulation are better for the spectral analysis of velocity

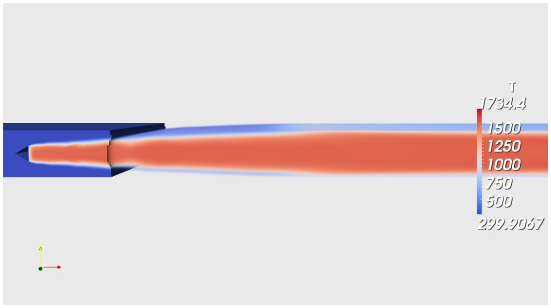

Figure 15. Profile of progress variable in $X/Xr = 0.35$

and energy, they have a better configuration for the tensors filters modeled in the SGS, and may perfectly show the inertial zone for the tensor cross, this does not happen in two-dimensional.

In the velocities case the comparisons with the experimental simulations are well approximated with a better performance in the longitudinal component, since the transverse component values are close to the experimental and are within the measurement error that establishes Sanquer.

6. ACKNOWLEDGEMENTS

The authors acknowledge the support from Laboratorio de Propulsão Liquida (LPL-IAE) of Instituto de Aronautica e Espaço for the use of the facilities to perform this work and CAPES for financial support.

7. REFERENCES

Bai, X. and Fuchs, L., 1994. "Modeling of turbulent reactive flows past a bluff body: Assessment of accuracy and efficiency". Computers and Fluids, Vol. 23, No. 3, pp. 507âĂŞ5211.

Candel, S., 1992. "Combustion instabilities coupled by pressure waves and their active control". *24th Symp.(Int.) on combustion. The Combustion Institute*, Vol. 24th Symposium, pp. 1277–1296.

Dourado, W.C., 2003. *Desenvolvimento de um método numérico em malhas não estructuradas hibridas para escoamentos turbulentos em baixo número de Mach: aplicação em chama propagando-se livremente e esteiras inertes e reativas*. Ph.D. thesis, ITA, SJC-SP.

Fureby, C., 2009. "Les modeling of combustion for propulsion applications". *Phil.Trans. R. Soc. A*, Vol. 367, p. 2957.

Fureby, C., Tabor, G. and Weller, H.G., 1997. "Differential subgrid stress models in large eddy simulations". *PHYS FLUIDS*, Vol. 9, pp. 3578–3580.

Grinstein, F.F. and Kailasanath, K.K., 1994. "Three dimensional numerical simulations of unsteady reactive square jets". *Comb. and Flame*, Vol. 100, p. 2.

Gulder, O.L., 1990. "Turbulent premixed flame propagation models for different combustion regimes". *Twenty-third Symposium (International) on Combustion. The Combustion Institute*, Vol. Twenty-third Symposium, pp. 743–750.

Jayatilleke, C., 1969. "The influence of prandtl number and surface roughness on the resistance of the laminar sublayer to momentum and heat transfer". *Prog. Heat Mass Transfer*, Vol. 1, pp. 193–321.

Peters, N., 2000. *Turbulent Combustion*. Cambridge University Press, Cambridge.

Porumbel, I., M.S., 2006. *Large Eddy Simulation of Bluff Body Stabilized Premixed Flame*. AIAA 2006-152, Cambridge.

Sanquer, S., 1998. *Experimental Study of a Buff-Body Wake, in Presence of Combustion, in Fully Developed Turbulent Channel Flow: Turbulence Scales and Critical Analysis of Transport and Combustion Models*. Ph.D. thesis, Universite de Poitiers, Potiers.

Sullerey, R.K., Gupta, A.K. and Moorthy, C.S., 1975. "Similarity in the turbulent near weak of bluff bodies". *AIAA Journal*, Vol. 13, No. (11), pp. 1425 – 1429.

Veynante, D., 2006. "Large eddy simulation of turbulent combustion". *Conference on Turbulence and Interaction*, Vol. TI2006, p. 20.

Weller, H.G., 1993. *The development of a new flame area combustion model using conditional averagingThermo-Fluids Section Report TF 9307*. Ph.D. thesis, Imperial College of Science, technology and Medicine, London.

Weller, H.G., Marooney, C.J. and Gosman, A.D., 1990. "A new spectral method for calculation of the time-varyng area of laminar flame in homogeneus turbulence". *Twenty-third Symposium (International) on Combustion, The combustion institute*, Vol. Twenty-third Symposium, pp. 629–636.

Weller, H.G. and Tabor, G., 2004. "Large eddy simulation of premixed turbulent combustion using xi flame surface wrinkling model". *flow,Turbulence and Combustion*, Vol. 72, pp. 1–28.

Weller, H.G., Tabor, G., Gosman, A. and Fureby, C., 1998. "Application of a flame-wrinkling les combustion model

to a turbulent mixing layer". *27th Symposium (International) on Combustion The combustion Institute*, Vol. 27th Symposium, pp. 899–907.

Wolf, P., Staffelbach, G., Roux, A., Gicquel, L., Poinsot, T. and Mourea, V., 2009. "Massively parallel les of azimuthal thermo-acoustic instabilities in annular gas turbines". *Comptes Rendus Mecanique*, Vol. 337, No. (6-7), pp. 385 – 394.

8. Responsibility notice

The author(s) is (are) the only responsible for the printed material included in this paper